An Efficient Method for Analyzing PAR Observed Tornadic Mesocyclones and Designing PAR Adaptive Scans

Qin Xu, *NOAA/National Severe Storms Laboratory, Norman, Oklahoma*
Li Wei and Kang Nai, *Cooperative Institute for Mesoscale Meteorological Studies, University of Oklahoma*

1. Introduction

A two-dimensional variational method was developed by Xu et al. (2015 *JTech*, X15) to analyze vortex wind fields of tornadic mesocyclones observed by operational WSR-88D radars for nowcast applications. In this method, the vortex wind field is retrieved in a nested domain over the mesocyclone area in a moving coordinate system co-centered the mesocyclone on the lowest sweep of radar scan. As the background error covariance is formulated with the desired vortex flow dependence, the method can retrieve the vortex winds of mesocyclones scanned from a single Doppler radar. To take the advantages provided by the rapid scans of phased array radar (PAR), the method is extended by including the advection equations of radar image pattern movements as additional constraints in the cost-function, so it can use PAR rapid scans on multiple consecutive time levels (instead of single time level) to extract additional information on vortex winds from image pattern movements. The extended method is described in the next section.

2. Extended method

As shown in (15)-(22) of X15, the background error covariance with the desired vortex flow dependence can be derived in the form of

$$\mathbf{B} = (\sigma_R\mathbf{P}, \sigma_T\mathbf{P})^{diag}(\sigma_R\mathbf{P}^T, \sigma_T\mathbf{P}^T)^{diag}, \quad (1)$$

where $\mathbf{B}^{1/2} \equiv (\sigma_R\mathbf{P}, \sigma_T\mathbf{P})^{diag}$ is a 2×2 block diagonal matrix satisfying $\mathbf{B}^{1/2}\mathbf{B}^{T/2} = \mathbf{B}$, σ_R^2 (or σ_T^2) is the background error variance for the radial-component (or tangential-component) velocity in the moving coordinate system co-centered the mesocyclone, and $\mathbf{P}$ is the square root of correlation matrix formulated by the vortex-flow-dependent correlation function. The method of X15 can be extended by incorporating $\mathbf{B}$ formulated in (1) into the simple adjoint (SA) method (Qiu and Xu 1992, *JTech*).

The SA method uses the reflectivity as a tracer, with its advection equation formulated as a weak constraint in the cost-function, to retrieve the wind field from radar scanned reflectivity pattern movements. The method was upgraded by using a recursive filter to efficiently compute the background error covariance, and the upgraded SA method was applied to PAR rapid scans of storm generated microbursts (Qiu et al. 2013, *Advances in Meteorology*). In the upgraded SA method, the cost-function has the following form:

$$J = |\mathbf{c}|^2 + \tau^{-1}\int dt|\mathbf{Hc}_- - \mathbf{d}|^2/\sigma_{ov}^2 + \tau^{-1}\int dt|\mathbf{F(c)} - \mathbf{y}|^2/(\sigma_F^2 + \sigma_o^2), \quad (2)$$

where $\mathbf{c} = (\mathbf{u}_c^T, \mathbf{v}_c^T, \mathbf{s}_c^T)^T$ is the control vector, $(\ )^T$ denotes the transpose of $(\ )$, $\mathbf{c}_- = (\mathbf{u}_c^T, \mathbf{v}_c^T)^T$, $\mathbf{H}$ (or $\mathbf{d}$) is the observation operator (or innovation vector) for radar-observed radial velocity, $\tau^{-1}\int dt(\ )$ denotes the time average of $(\ )$ over τ – the analysis time window, σ_{ov}^2 is the radial-velocity observation error variance, $\mathbf{F}(\ )$ denotes the observation operator that uses $\mathbf{c}$ to integrate the reflectivity advection equation, $\mathbf{y}$ is the observation vector for radar-observed reflectivity, σ_F^2 is the error variance for $\mathbf{F}(\ )$, and σ_o^2 is the reflectivity observation error variance. The three component vectors of $\mathbf{c}$ in (2) are subject to the following transformations:

$$\mathbf{u}_a = \sigma_b\mathbf{Gu}_c, \ \mathbf{v}_a = \sigma_b\mathbf{Gv}_c, \ \mathbf{s}_a = \sigma_s\mathbf{G}_s\mathbf{s}_c, \quad (3)$$

where $\mathbf{u}_a$ (or $\mathbf{v}_a$) is the state vector of analyzed time-mean velocity incremental field Δu (or Δv), $\mathbf{s}_a$ is the state vector of analyzed time-mean source field S in the reflectivity advection equation, σ_b^2 (or σ_s^2) is the background error variance for Δu or Δv (or S), and $\mathbf{G}$ (or $\mathbf{G}_s$) is the square root of background error correlation matrix for Δu or Δv (or S) modeled by an isotropic Gaussian function and computed by a recursive filter.

When $\mathbf{B}$ in (1) is incorporated into (2), $\mathbf{c}$ is expended to $\mathbf{c} = (\mathbf{c}_R^T, \mathbf{c}_T^T, \mathbf{c}_s^T, \mathbf{u}_c^T, \mathbf{v}_c^T, \mathbf{s}_c^T)^T$ with the three new component vectors subject to the following transformations:

$$\mathbf{a}_R = \sigma_R\mathbf{Pc}_R, \ \mathbf{a}_T = \sigma_T\mathbf{Pc}_T, \ \mathbf{s}_+ = \sigma_s\mathbf{P}_s\mathbf{c}_s, \quad (4)$$

$$(\mathbf{u}_+^T, \mathbf{v}_+^T)^T = [(\mathbf{\Lambda}_c, -\mathbf{\Lambda}_s)^T, (\mathbf{\Lambda}_s, \mathbf{\Lambda}_c)^T](\mathbf{a}_R^T, \mathbf{a}_T^T)^T, \quad (5)$$

where $\mathbf{a}_R$ (or $\mathbf{a}_T$) is the state vector of the time-mean vortex-relative radial (or tangential) velocity incremental field, $\mathbf{u}_+$ (or $\mathbf{v}_+$) is the new component for the state vector of Δu (or Δv), and $\mathbf{\Lambda}_c$ and $\mathbf{\Lambda}_s$ are diagonal matrices for the transformation in (5) [see (11) of X15]. The state vectors computed from the new control vector components are combined with those in (3) as follows:

$$\mathbf{u} = \mathbf{\Lambda u}_+ + (\mathbf{I} - \mathbf{\Lambda})\mathbf{u}_a, \ \mathbf{v} = \mathbf{\Lambda v}_+ + (\mathbf{I} - \mathbf{\Lambda})\mathbf{v}_a, \ \mathbf{s} = \mathbf{\Lambda s}_+ + (\mathbf{I} - \mathbf{\Lambda})\mathbf{s}_a,$$

where $\mathbf{\Lambda}$ is a diagonal matrix with its diagonal elements given between 0 and 1 as a smooth function of (x, y). For simplicity, we set $\mathbf{\Lambda} = \lambda\mathbf{I}$ with $1 \geq \lambda \geq 0$. For $\lambda = 1$, $\mathbf{B}$ in (1) is fully incorporated into (2). For $\lambda = 0$, the method reduces to the SA method.

3. Application to PAR scanned tornadic mesocyclone

The extended method is applied to NSSL PAR scans (from 19:52 to 20:35 UTC) of the tornadic mesocyclone that struck Moore in Oklahoma on 20 May 2013. Examples of retrieved vortex wind fields are shown in Fig. 1a for the extended method ($\lambda = 1$) and Fig. 1b for the SA method ($\lambda = 0$). The vortex wind field retrieved by the extended method in Fig. 1a appears more accurate than that by the SA method in Fig. 1b, as the former compares better (than the latter) with the dual-Doppler retrieved vortex wind field (not shown) from PAR and operational KTLX scans, especially in the vortex core area and around the curved convergence zone to the southeast side of the vortex. To test the method quantitatively, model-simulated vortex wind and reflectivity fields are used in the next section, and simulated PAR radial-velocity observations are also used as a trace field [with its advection equation added to J similarly to the last term in (2) for the reflectivity tracer].

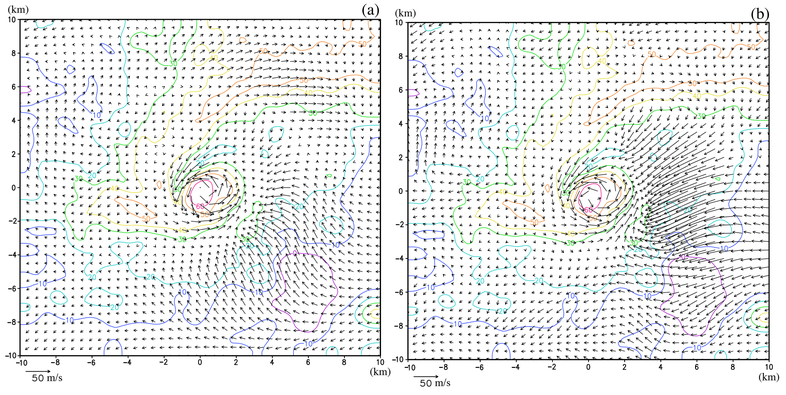

Fig. 1. Time-mean vortex winds (plotted by arrows) retrieved in a moving coordinate system co-centered with the vortex on the conical surface of 0.5° sweep by (a) the extended method ($\lambda = 1$) and (b) SA method ($\lambda = 0$) from three consecutive PAR scans of Oklahoma Moore tornadic mesocyclone at 20:04:40, 20:06:17 and 20:07:27 UTC on 20 May 2013. The color contours plot the reflectivity (in dBz).

4. Tests with model-simulated tornadic mesocyclone

Model-simulated vortex wind and reflectivity fields (saved every 10 s) are used to generate simulated PAR radial-velocity and reflectivity observations over each selected time period τ. Fig. 2a plots simulated true vortex winds (black arrows) averaged over τ = 60 s in the moving coordinate system co-centered with the vortex at 0.2 km height. Fig. 2b plots the retrieved time-mean vortex winds (black arrows) versus those (duplicated by green arrows) in Fig. 1a. The RMS error of the retrieved vortex winds in Fig. 2b is listed (4.59 m/s) in Table 1 versus the RMS errors obtained by using 0, 1 or 2 traces with λ= 0, 0.5 or 1. As listed, the RMS error can be reduced by using tracers (reflectivity and/or radial-velocity) and $\mathbf{B}$ in (1) (λ = 1 or 0.5).

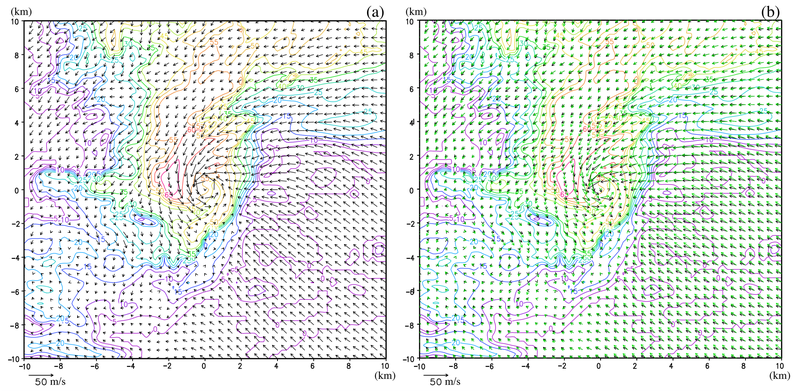

Fig. 2. (a) True vortex winds (black arrows) averaged over τ = 60 s. (b) Retrieved time-mean vortex winds (black arrows) versus the truth (green arrows) in (a). The vortex winds in (b) are retrieved by the extended method (λ = 1) from simulated PAR radial-velocity and reflectivity scans (from the east at 0.2 km height) every $\Delta\tau$ = 10 s over τ = 60 s. The color contours plot the reflectivity (in dBz).

Table 1. RMS errors (m/s) of vortex winds retrieved by using 0, 1 or 2 traces with λ= 0, 0.5 or 1.

	no tracer	1 tracer	2 tracers
$\lambda = 0$	7.55	5.58	5.10
$\lambda = 0.5$	6.20	5.31	4.59
$\lambda = 1$	5.87	5.65	5.02

5. Rapid adaptive scans for vortex wind analyses

The RMS errors of vortex winds retrieved by using 2 traces with different settings of τ and $\Delta\tau$ are listed in Table 2. As listed, the RMS error can be reduced if the scan rate is increased (from every 60 s to 30 s and 10 s) especially for τ = 60 s. Increasing the scan rate adaptively (to every $\Delta\tau$ = 10 s) can also reduce the location error of the estimated vortex center especially when the movement (or trajectory) of the true vortex center is highly unsteady (or curved). These results can be useful for designing PAR rapid scans adaptively for real-time vortex wind analyses.

Table 2. RMS errors of vortex winds retrieved by using 2 traces with different settings of τ and $\Delta\tau$.

	$\Delta\tau$ = 10 s	$\Delta\tau$ = 30 s	$\Delta\tau$ = 60 s
τ = 30 s	5.24	5.31	–
τ = 60 s	4.59	4.68	5.09
τ = 120 s	4.74	4.81	4.95